

## INFLUENCE OF DIFFERENT FATIGUE LOADING METHOD ON THE PROPERTY OF METAL CANTILEVER BEAM

Wei Cui<sup>1</sup>, Dingni He<sup>1</sup>, Jianjian Yu<sup>1</sup> and Yunfei Liao<sup>2</sup>

<sup>1</sup> China Helicopter Research and Development Institute, [cuiwei\\_buaa@163.com](mailto:cuiwei_buaa@163.com)

<sup>2</sup> Shanghai Aeronautical Materials & Structures Testing Co., LTD

**Abstract:** In order to investigate the influence of different fatigue loading methods on the property of metal cantilever, the resonant fatigue testing system and the corresponding conventional fatigue testing system were designed respectively based on the electromagnetic shaker table, and the bending fatigue tests were conducted on LY12CZ aluminium alloy cantilever beam specimens. A special progressive fitting analysis based on damage equivalence was used to obtain *S-N* curves under resonance environment in the range of  $1 \times 10^5$ - $1 \times 10^7$  cycles. The results show that the fatigue limit of LY12CZ aluminium alloy under bending resonance environment is very close to the fatigue limit under conventional condition at  $1 \times 10^7$  cycles. When the number of cycles is less than  $5 \times 10^6$ , the bending resonant fatigue property of LY12CZ aluminium alloy is significantly different from the conventional fatigue property, while in the range of  $5 \times 10^6$ - $1 \times 10^7$  cycles, there is little difference between the two properties.

**Keywords:** Resonant fatigue, Conventional fatigue, Cantilever beam, Fatigue Property

### 1. INTRODUCTION

During aircraft flight, some structures always work in strong excitation environments, such as jet noise, rotor excitation, etc. The damage caused by vibration fatigue in helicopter structures often exhibits characteristics of low load levels and abnormal fracture modes. These failures often occur on secondary and non-load bearing structures, such as fairing, access cover hinges, etc. In 1963, Crandall proposed the concept of vibration fatigue [1], which is the problem of fatigue failure of materials under the action of vibration loads. The most important characteristic of vibration fatigue is that the natural frequency of a structure in a resonant state changes after fatigue damage occurs. The key issue is to adopt suitable methods to simulate complex vibration environment. In order to analyze the fatigue life of helicopter secondary load-bearing structures under resonance conditions, it is necessary to obtain the fatigue performance of the materials through suitable test methods.

Fatigue analysis can be generally categorized into conventional fatigue analysis and resonant fatigue analysis. Vibration loads generally excite the bending modes of these structures. Resonant fatigue test of cantilever beam is one of the most widely used methods in engineering to obtain fatigue characteristics. When the vibration excitation is at a constant amplitude and a fixed frequency, the vibration response of the structure changes with the change of natural frequency. So far, the commonly used test methods for vibration fatigue test include: narrow-band random, resonance research and fixed frequency dwell, resonance research and tracking dwell (RSTD), etc. After

Crandall's work, a large number of experimental studies on the vibration fatigue performance of cantilever beams have been carried out. [2-10]. In 2009, Meng et al. [11] estimated the fatigue life of vibrating components under random vibration loads based on the power spectral density function (PSD), Pothula et al. [12] used random vibration method to study the fatigue life of aluminum alloy beams with different damping materials. Yang Qiang et al. [13] used vibrating table to apply a narrow band random excitation load to carry out a study on the vibration fatigue characteristics of engine composite blades. In 2018, Wu [14] used the RSTD to study the vibration fatigue of the titanium alloy hollow structure, and the correctness of the method was verified by the comparison of numerical analysis and experimental test.

The RSTD method is suitable for studying the fatigue characteristics of cantilever beams at a certain frequency. It is necessary to investigate the changes in the transfer function when fatigue damage occurs. The stress data processing methods in the S-N curve of vibration fatigue must be studied. Therefore, exploring the effects of two different fatigue loading methods, resonant fatigue and conventional fatigue, on the performance of metal cantilever beams has become a problem to be solved. In this paper, based on a shaker table, bending resonant fatigue and corresponding conventional fatigue tests were conducted on LY12CZ aluminium alloy cantilever beams. Based on the test results, the differences in fatigue performance of LY12CZ aluminium alloy cantilever beams under two types of loading were compared and analyzed.

## 2. EXPERIMENTAL DETAILS

### 2.1 Specimen design

Fatigue test is a basic method to obtain material fatigue property. Many fatigue testing methods have standard specifications such as ASTM, ISO, HB, industrial standards or other testing standards. In this paper, the specimen shown in Figure 1 is designed according to the Chinese aviation standard HB 5277-84 [15]. The specimen is made of LY12CZ aluminium alloy, a typical material used in aviation, with a Young's modulus of 72GPa, a density of 2780kg/m<sup>3</sup>, a yield strength of 393MPa, an ultimate tension strength of 496MPa and a Poisson's ratio of 0.27 according to the AMS 4050J. The 5.5mm diameter hole in the specimen is used to fix the counterweight and accelerometer under resonant environment and to apply loads in conventional fatigue test.

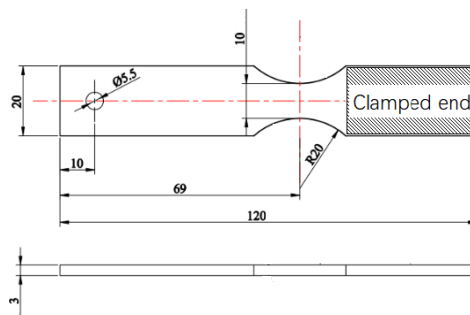


Figure 1: Dimensions of specimen in mm.

### 2.2 Resonant fatigue testing system

The resonant fatigue testing system used in this paper is composed of a vibration controller, an electromagnetic shaker table, a power amplifier, measurement and control system (a computer, some accelerometers, etc.), as shown in Figure 2. The smooth and notched specimens are installed on the fixture with bolts, ensuring that the clamped end is fixed and restrained, and that the fixture is installed on the slip table (see Figure 3). The specimens are excited by an electromagnetic shaker table in the direction along their thickness.

The resonant fatigue test is to obtain the material properties under the premise of resonance of the specimen. Therefore, it is necessary to obtain the natural frequency of the specimen under the

corresponding modal shape, and the resonance condition can be reached by using this natural frequency for test excitation. Based on the fundamental principle of modal analysis, the method of force-hammer excitation was adopted to conduct modal testing. The boundary condition of the specimen was consistent with that in Figure 3, and displacement sensors were arranged at appropriate positions of the specimen. The displacement data of the measuring points were imported into the modal analysis and processing system software by force-hammer excitation method to extract the modal parameters. The results of modal testing show that the first-order bending modal frequency is 79Hz.

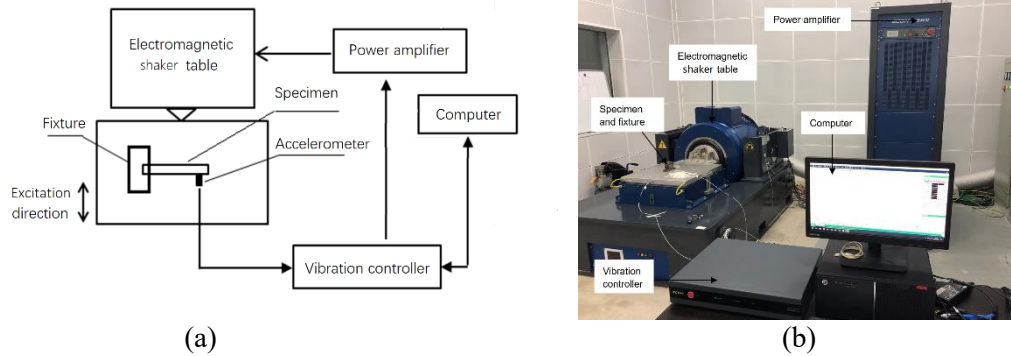


Figure 2 (a)-(b): Schematic diagram and physical diagram of the resonant fatigue testing system.

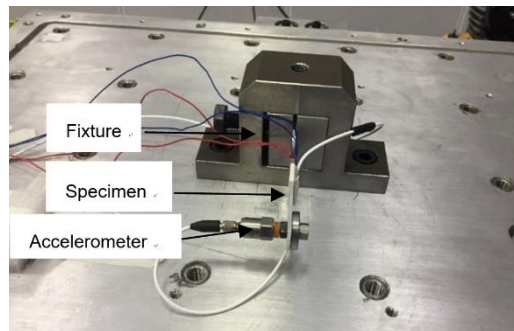


Figure 3: Installation drawing of specimen and fixture.

A strain gauge is attached to the minimum cross-sectional area of the specimen, and a counterweight sheet as well as a response accelerometer is arranged at the end of the specimen. Ensure the level state of the specimen during installation. Before the test, the relationship between response acceleration and strain was calibrated through base excitation. The response of calibration target started from 40g, the difference in target response level was 10g, and the calibration ended at 120g. The mean value of strain collected at each level was converted into stress through formula  $\sigma = E \cdot \varepsilon$ . The stress on the danger zone is characterized by response acceleration instead of strain value, through which the damage of strain gauge caused by the deformation of the danger zone can be avoided and the reliability of data can be ensured. The initial excitation acceleration is determined according to the stress level of the dangerous point, which is kept unchanged during the test. In order to ensure that the specimen is always in the first-order resonance state, the resonance dwell method is adopted in the testing system, that is, the phase difference between the excitation acceleration and the response acceleration is guaranteed to be  $90^\circ$  by the control program. Stress ratio is -1 through this testing method. The acceleration of the shaker table was controlled as a constant value in order to maintain the input excitation during the resonant fatigue test. The parameters monitored during the resonant fatigue test are response acceleration and frequency. Based on HB 5277-84 [15] and a large number of previous experimental studies, it has been found that when the natural frequency of specimen decreased by 2%, the specimen was close to the fracture state, cracks can be found by stereomicroscope, and obvious detectable cracks or fracture would occur rapidly after continued loading. Therefore, the stopping criterion of the resonant fatigue test is that the response acceleration drops sharply, the natural frequency drops by more than 2%, or the cycle number reaches  $10^7$  cycles.

Considering the dynamic characteristics of the specimen during the resonant fatigue test, as the test proceeds, the natural frequency of the specimen will decrease, and the response acceleration will change, leading to continuous changes in the true stress of the danger zone of the specimen. Therefore, during the test, it is also necessary to continuously record the corresponding response acceleration and cycles when the natural frequency decreases.

### 2.3 Conventional fatigue testing system

In order to carry out a comparative analysis and research on the bending resonant fatigue and the corresponding conventional fatigue properties of the specimens, a conventional fatigue testing system is designed based on the resonant fatigue testing system, as shown in Figure 4. A push rod is used in the system to connect the end of the specimens, which is of smooth and notched types respectively. The specimens are installed on a fixture (shown as Figure 5), and the loads along the thickness direction of the specimens are applied by controlling the displacement of the electromagnetic shaker table.

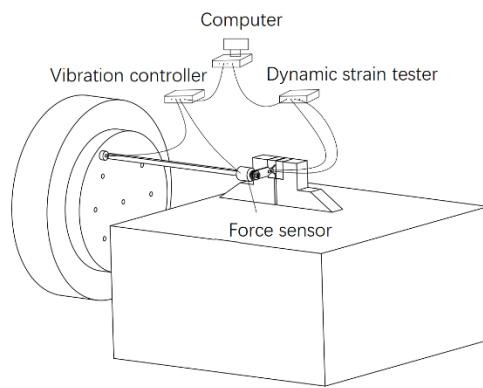


Figure 4: Schematic diagram of the conventional fatigue testing system.

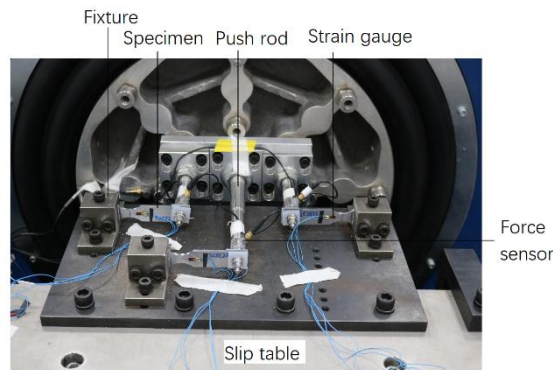


Figure 5: Installation drawing of specimen and the fixture.

A strain gauge is attached to the minimum cross-sectional area of the specimen, and a push rod as well as force sensor is arranged at the end of the specimen. During the installation, the level of the specimen is first guaranteed by a cushion block, and then the fixture and the clamped end of the specimen are tightened with bolts to ensure that the specimen is fixed constraint. After removing the cushion block, no additional bending moment will exist during the test. Before the test, the relationship between the input displacement peak value and strain value was calibrated based on the input displacement of the electromagnetic shaker table, and the displacement peak value-stress curve was obtained. The input displacement peak is determined according to the stress level at the dangerous point, which is kept unchanged during the test, and the stress ratio is consistent with that of the vibration fatigue test ( $R=-1$ ). The loading frequency is 20Hz. The parameter monitored during the conventional fatigue tests is force. When cracks occur in the danger zone of the specimens, their

response force drops sharply. Therefore, the sharp decline of response force of the specimens, the cracks of the specimens or the cycle number reaching  $10^7$  cycles are taken as the stopping criterion of the conventional fatigue tests.

### 3. PROGRESSIVE FITTING METHOD

In this paper, both conventional fatigue and resonant fatigue tests are conducted with consistent input loads. Conventional fatigue can be considered as constant amplitude cyclic loading, and the true stress in the danger zone of the specimen remains unchanged. Resonant fatigue considers the dynamic characteristics of the specimen, and the true stress of the danger zone will change during the test, which can be considered as variable amplitude cyclic loading. Palmgren and Miner have independently proposed a linear damage accumulation theory for fatigue failure, which can quantitatively evaluate the impact of different stress levels on fatigue life, known as Palmgren-Miner accumulated fatigue damage rule. In this paper, based on the true stress value of the danger zone of the specimen in the resonant fatigue test, based on Palmgren-Miner accumulated fatigue damage rule, and according to the damage equivalence principle, a progressive fitting analysis is performed to obtain the true  $S$ - $N$  curve of the resonant fatigue test.

The progressive fitting process is as follows:

i) The initial fitting  $S$ - $N$  curve is obtained by fitting the group method and up-and-down method data of the excitation acceleration corresponding to the stress level. The expression of  $S$ - $N$  curve of the specimens is usually given by the power function fitting of three parameter [13]:

$$\lg N = a_0 - b_0 \times \lg(S_{\max} - S_{\infty 0}) \quad (1)$$

where,  $a_0$  and  $b_0$  are material parameters, which varies according to the material and state of the specimen,  $S_{\infty 0}$  is the corresponding material fatigue limit when the number of cycles is infinite,  $N$  is failure life, and  $S_{\max}$  is the maximum stress, here is the initial danger zone stress.

ii) For the specimen with serial number 1, the cycle of tests recorded under constant amplitude cyclic stress  $S_i$  is  $n_i$ . According to Eq. (1), the fatigue life under this stress  $S_i$  is  $N_i(S_i)$ , and the damage  $D_i(S_i)$  suffered after undergoing  $n_i$  cycles at this stress level  $S_i$  can be defined as

$$D_i(S_i) = \frac{n_i}{N_i(S_i)} \quad (2)$$

When the specimen is cycled to failure, a total of  $k$  stress levels  $S_i$  are recorded for cycles  $n_i$ , and the total damage  $D_1$  sustained by it can be defined as

$$D_1 = \sum_{i=1}^k D_i(S_i) = \sum_{i=1}^k \frac{n_i}{N_i(S_i)} \quad (3)$$

According to Eq. (1), the fatigue life of the equivalent true stress  $S_{a1}$  of serial number 1 specimen is  $N(S_{a1})$ , and the damage under the total number of cycles can be defined as

$$D_{a1} = \frac{\sum_{i=1}^k n_i}{N(S_{a1})} \quad (4)$$

According to the damage equivalence principle  $D_I = D_{at}$ , the equivalent true stress  $S_{at}$  of serial number 1 specimen can be obtained. Similarly, the corresponding equivalent stress of the remaining specimens can be obtained, and the first iteration  $S-N$  curve of the response can be obtained by using the group method and the up-and-down method of the equivalent stress level.

iii) According to the first iteration  $S-N$  curve, step ii) can be repeated, and the equivalent stress can be obtained by using the damage equivalent method again for each specimen, and then the second iteration  $S-N$  curve can be obtained, as well as the third to the  $N$ th iteration  $S-N$  curve.

iv) The end of the progressive fitting analysis is controlled based on the error between the conditional fatigue limit at  $1 \times 10^7$  cycles obtained from the  $N$ th iteration and the  $N-1$ th iteration is less than 0.5%.

## 4. RESULTS

### 4.1 Resonant fatigue testing results

A total of 27 effective specimens were completed in the resonant fatigue tests, including 15 pieces at 3 stress levels through grouped method and 12 pieces through up-and-down method, and the test results are shown in Table 1. In the process of the bending resonant fatigue test, the excitation acceleration was always kept unchanged. According to the calibration relationship of  $a-\sigma$  curve before the test, the excitation acceleration was converted to the initial danger zone stress, and the stress level of the specimens was characterized by the initial danger zone stress.

Table 1: Resonant fatigue testing results.

Serial number	Initial danger zone stress (MPa)	Number of cycles	Serial number	Initial danger zone stress (MPa)	Number of cycles
1	164	79219	15	85	339745
2	164	89670	16	69	2699658
3	164	86604	17	69	3412632
4	96	264362	18	69	6835095
5	96	270293	19	66	5620226
6	96	314057	20	66	9720195
7	96	281502	21	66	7208300
8	85	501220	22	66	>10000000
9	85	401152	23	66	>10000000
10	85	641353	24	66	>10000000
11	85	560013	25	62	>10000000
12	85	464399	26	62	>10000000
13	85	502707	27	62	>10000000
14	85	469406	-	-	-

Taking the serial number 4 in Table 1 as an example, the response acceleration and true danger zone stress obtained from  $a-\sigma$  curve as well as cycles corresponding to the natural frequency drop recorded during the test are shown in Table 2.

Table 2: Test process record of individual specimen.

Frequency drop value (Hz)	Response acceleration (g)	True danger zone stress (MPa)	Number of cycles
0.0	45.4	96.9	31393
0.1	45.7	97.5	70189
0.3	45.9	97.9	100906
0.5	46.7	99.6	134801
0.9	48.1	102.6	170358
1.3	49.9	106.5	210280
1.7	51.6	110.1	240916
2.0	52.6	112.2	264362

#### 4.2 Conventional fatigue testing results

A total of 22 effective specimens were completed in the conventional fatigue tests, including 14 pieces at 3 stress levels through grouped method and 8 pieces through up-and-down method, and the test results are shown in Table 2. During the bending conventional fatigue test, the peak of excitation displacement was kept unchanged. According to the calibration relation of  $P$ - $\sigma$  curve before the test, the peak of excitation displacement was converted to the initial danger zone stress. Consistent with the resonant fatigue test, the stress level of the specimens is characterized by the initial danger zone stress.

Table 3: Conventional fatigue testing results.

Serial number	Initial danger zone stress (MPa)	Number of cycles	Serial number	Initial danger zone stress (MPa)	Number of cycles
1	170.6	121340	12	99.5	620790
2	170.6	161836	13	99.5	705073
3	170.6	108735	14	99.5	661185
4	170.6	114664	15	80.7	2322847
5	170.6	134923	16	77.1	2334194
6	145	230925	17	77.1	1122532
7	145	166449	18	77.1	>10000000
8	145	225000	19	73.6	>10000000
9	145	231720	20	77.1	1122532
10	145	225000	21	73.6	>10000000
11	99.5	737775	22	73.6	>10000000

#### 4.3 Fatigue fracture morphology

The specimen that has not yet completely broken (but has reached the failure criterion) in the test process was stretched along the vertical direction of the crack using an electronic universal testing machine, and the tensile process was based on the principle of not damaging the fracture surface. Then, ultrasonic cleaning was performed on all fractures, and the fracture morphology was observed under the stereomicroscope, as shown in Figure 6. Although the fatigue crack growth history is different, the low magnification fracture morphology of the sample shows that it is mainly composed of three areas: fatigue crack initiation site, crack propagation region and fast fracture zone (the vibration fatigue specimen has not been tested to fracture, so the fast fracture zone is not obvious, as shown in Figure 6 (b)).

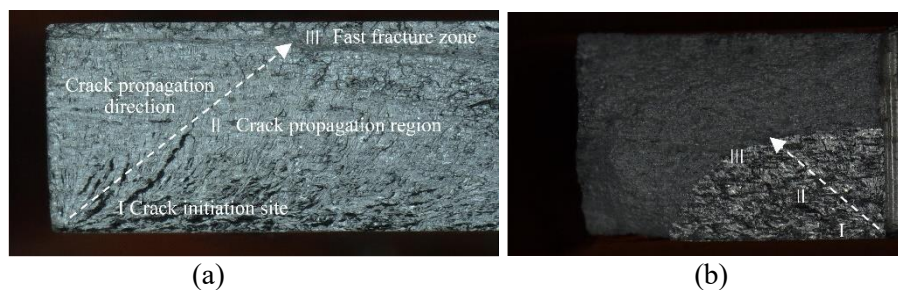
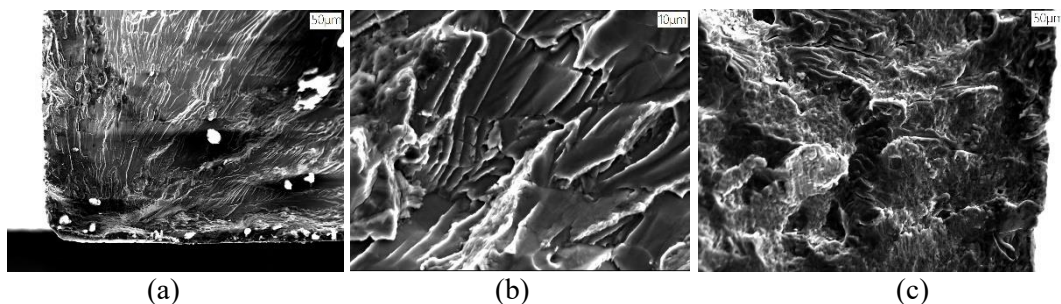


Figure 6 (a)-(b): Fracture morphology of conventional fatigue and vibration fatigue specimens.



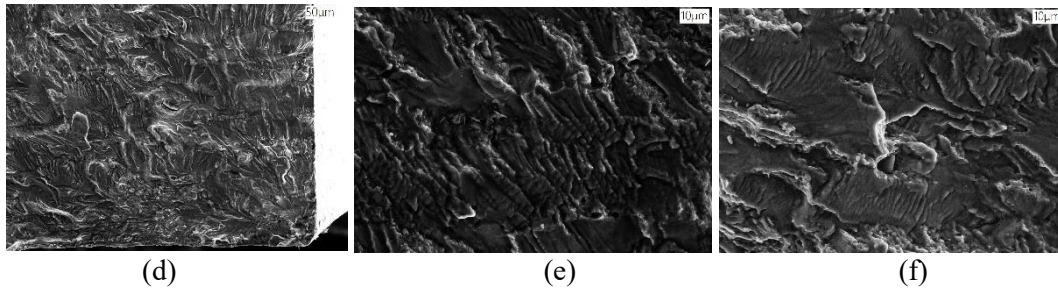


Figure 7 (a)-(c): Crack initiation site, crack propagation region and fast fracture zone of conventional fatigue specimen under SEM; (d)-(f): crack initiation site, crack propagation region and fast fracture zone of resonant fatigue specimen under SEM.

Figure 7 shows the SEM photos of the fatigue fracture morphology. The SEM analysis shows that there is transgranular fracture near the crack initiation site, a large number of fatigue bands can be observed in the crack propagation region, there are diffusion prisms converging to the initial position of the crack in the fast fracture zone, the crack surface is relatively flat, and there are many parallel fatigue stripes on the crack surface. It can be seen that the fracture mechanism under bending resonant fatigue environment is roughly the same as that under bending conventional fatigue loading.

## 5. DISCUSSION

The test data of specimens under resonant and conventional fatigue loading is fitted respectively. At the same time, five iterations of the resonant fatigue test data were performed using the progressive fitting method, and the iteration program was terminated. The results in Table 4 were obtained. According to the data fitting results, the resonant and conventional fatigue  $S-N$  curves of LY12CZ aluminium alloy are drawn, as shown in Figure 8.

Table 4: Fitting results of  $S-N$  curve parameters.

Curve form	$\lg N = a - b \times \lg(S_{\max} - S_{\infty})$		
	$a$	$b$	$S_{\infty}$ (MPa)
Conventional fatigue test curve	7.6254	1.2546	73.0831
Initial curve of resonant fatigue test	7.0812	1.0790	64.5609
First iteration curve of resonant fatigue test	7.1049	1.0797	71.1955
Second iteration curve of resonant fatigue test	6.9712	1.0184	73.6482
...	...	...	...
Fifth iteration curve of resonant fatigue test	6.8418	0.9588	75.4536

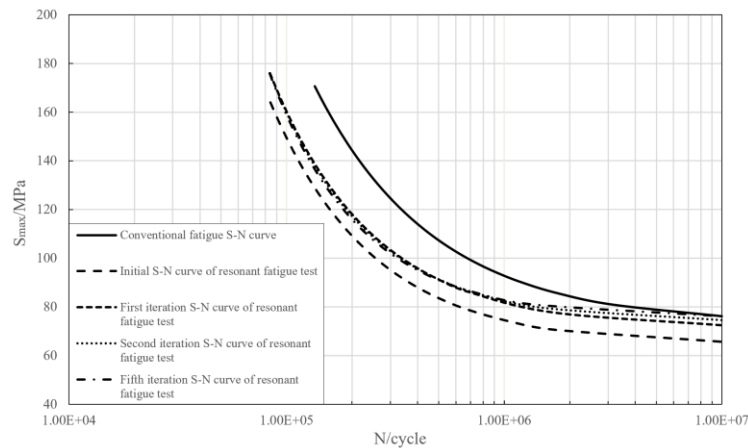


Figure 8: Resonant fatigue and conventional fatigue  $S-N$  curves of LY12CZ aluminium alloy.

As can be seen from Figure 8, in the range of  $10^5$ - $10^7$  cycles, the  $S$ - $N$  curves of LY12CZ aluminium alloy show a continuously downward trend with the increase of cycle number, and there are obvious horizontal progressive platforms or fatigue limits. Fatigue limits comparison between resonant and conventional  $S$ - $N$  curves are listed, as shown in Table 5.

Table 5: Fatigue limits comparison between resonant and conventional  $S$ - $N$  curves.

Number of cycles	Fatigue limits $S_{\infty}$		
	Conventional fatigue $S_{\infty,C}$ (MPa)	Resonant fatigue $S_{\infty,R}$ (MPa)	Relative difference $\frac{S_{\infty,R} - S_{\infty,C}}{S_{\infty,C}}$ (%)
$2 \times 10^5$	144.32	115.90	-19.69
$5 \times 10^5$	107.40	91.01	-15.26
$8 \times 10^5$	96.68	84.98	-12.10
$1 \times 10^6$	92.83	83.00	-10.59
$2 \times 10^6$	84.45	79.12	-6.31
$5 \times 10^6$	78.56	76.86	-2.16
$8 \times 10^6$	76.85	76.32	-0.69
$1 \times 10^7$	76.23	76.14	-0.12

The initial  $S$ - $N$  curve obtained from resonant fatigue test is significantly different from the  $S$ - $N$  curve obtained from conventional fatigue test. The fatigue limit corresponding to  $2 \times 10^5$  cycles in the resonant fatigue  $S$ - $N$  curve is 19.69% lower than the fatigue limit of in the conventional fatigue  $S$ - $N$  curve. However, the progressive iterative curve obtained by characterizing resonant fatigue using the true stress of the danger zone is relatively close to the conventional fatigue  $S$ - $N$  curve, especially as the number of cycles increases, the curves under the two loading methods gradually approach. The relative difference is -0.12% between the resonant and conventional fatigue limits at  $1 \times 10^7$  cycles.

The stress amplitude corresponding to a certain cycle number is defined as the conditional fatigue limit for a continuous descending  $S$ - $N$  curve. At  $1 \times 10^7$  cycles, the conditional fatigue limit under resonant fatigue loading is 76.14MPa. The conditional fatigue limit under conventional fatigue loading is 76.23MPa. The relative difference is -0.12%. Therefore, the fatigue properties of LY12CZ aluminium alloy under resonant or conventional loads are close to each other.

It can also be concluded from Figure 8 and Table 5 that, for the resonant and conventional fatigue  $S$ - $N$  curves, when the number of cycles is less than  $5 \times 10^6$ , the bending resonant fatigue property of LY12CZ aluminium alloy is significantly different from the conventional fatigue property, while in the range of  $5 \times 10^6$ - $1 \times 10^7$  cycles, there is little difference between the two properties. Therefore, it can be considered that when the structure is under resonant fatigue and conventional fatigue, the two loading methods have little impact on the fatigue property at  $10^7$  cycles which is commonly used in engineering, but the shape parameters of the  $S$ - $N$  curve are slightly different.

## 6. CONCLUSIONS

In this paper, both resonant and conventional fatigue tests on specimens of LY12CZ aluminium alloy have been carried out to investigate the fatigue property under different fatigue loading methods, and the fatigue property was characterized by using the true stress of the danger zone using the progressive fitting method. The main conclusions are summarized as follows:

- i) From the fracture surface of the specimen, it can be seen that the fracture mechanism under bending resonant fatigue environment is roughly the same as that under bending conventional fatigue loading.
- ii) The fatigue limit of LY12CZ aluminium alloy under bending resonance environment is very close to the fatigue limit under conventional condition at  $1 \times 10^7$  cycles.

iii) When the number of cycles is less than  $5 \times 10^6$ , the bending resonant fatigue property of LY12CZ aluminium alloy is significantly different from the conventional fatigue property, while in the range of  $5 \times 10^6$ - $1 \times 10^7$  cycles, there is little difference between the two properties.

## REFERENCES

- [1] Crandall S H. (1963), Zero crossings, peaks, and other statistical measures of random responses. *J. Acoust. Soc. Am.*, vol. 34, n. 12, pp. 1693-1699.
- [2] Wozney, G. P. (1962), Resonant-vibration fatigue testing. *Experimental Mechanics*, vol. 2, n. 1, pp. 1-8.
- [3] To, C. W. S. (1982), Vibration of a cantilever beam with a base excitation and tip mass, *J. Sound Vib.*, vol. 83, no. 4, pp. 445-460, 1982.
- [4] Cartmell, M. and Roberts, J. (1987), Simultaneous combination resonances in a parametrically excited cantilever beam, *Strain*, vol. 23, no. 3, pp. 117-126.
- [5] Jaworski, J. and Dowell, E. (2008), Free vibration of a cantilevered beam with multiple steps: comparison of several theoretical methods with experiment, *Journal of Sound and Vibration*, vol. 312, no. 4-5, pp. 713-725.
- [6] Liu, W. G. and Chen, G. P. (2011), Coupling analysis for vibration and fatigue of a cracked cantilever beam. *J. Vib. Shock*, vol. 30, n. 5, pp. 140-144.
- [7] Paulus, M., Dasgupta, A. and E. Habtour, E. (2012), Life estimation model of a cantilevered beam subjected to complex random vibration, *Fatigue and Fracture of Engineering Materials and Structures*, vol. 35, no. 11, pp. 1058-1070.
- [8] Tang, Z. J., Shi, Z. F. and Hu, H. T. (2012), Fatigue Properties of LY12 Cantilever Beam under Different Vibration Frequencies. *J. Mater. Sci. Eng.*, vol. 3, n. 1, pp. 110-122.
- [9] Habtour, E., Connon, W., Pohland, M., Stanton, S., Paulus, M. and Dasgupta, A. (2014), Review of response and damage of linear and nonlinear systems under multiaxial vibration. *Shock Vib.*, vol. 2014, n. 1, pp: 1-21.
- [10] Liu, W. G. and Wang, Y. W. (2020), Fatigue crack growth life prediction for a notched beam based on modal frequency. *J. Vib. Shock*, vol. 39, n. 1, pp. 102-108.
- [11] Meng, C. R. and Lu, B. Y. (2009), Estimation on vibration fatigue life-span under random loading based on PSD. *J. Machine Design*, vol. 26, n. 5, pp. 73
- [12] Pothula, A., Gupta, A. and Kathawate, G. R. (2012), Fatigue failure in random vibration and accelerated testing. *J. Vib. Control*, vol.18, n. 8, pp. 1199-1206.
- [13] Yang, Q., Shao, C. and Fang, K. Q. (2014), Vibration fatigue characteristics study of aeroengine composite blade. *J. Experimental Mechanics*. vol. 29, n. 3, pp. 362-367.
- [14] Wu, Q., Deng Y. and Deng W. J. (2018), Research of high cycle fatigue test on complex structures of titanium alloy. *Aeronautical Manufacturing Technol.*, vol. 61, n. 10, pp. 90-103.
- [15] HB5277 (1984): Vibration fatigue test method for engine blades and materials, *Chinese Aviation Standards*.